Peptide Models of the Helical Hydrophobic Transmembrane Segments of Membrane Proteins: Interactions of Acetyl-K_2-$(LA)_{12}$-K_2-Amide with Phosphatidylethanolamine Bilayer Membranes†

Yuan-Peng Zhang, Ruthven N. A. H. Lewis, Robert S. Hodges, and Ronald N. McElhaney*

Department of Biochemistry, University of Alberta, Edmonton, Alberta, Canada T6G 2H7

Received September 15, 2000; Revised Manuscript Received October 26, 2000

ABSTRACT: High-sensitivity differential scanning calorimetry (DSC) and Fourier transform infrared (FTIR) spectroscopy were used to study the interaction of a synthetic α-helical hydrophobic transmembrane peptide, acetyl-Lys_2−(Leu−Ala)$_{12}$−Lys_2-amide [$(LA)_{12}$], and members of a homologous series of *n*-saturated diacylphosphatidylethanolamines (PEs). In the lower range of peptide mole fractions, the DSC endotherms exhibited by the lipid/peptide mixtures consist of two components. The temperature and cooperativity of the sharper, higher temperature component are very similar to those of pure PE bilayers and are almost unaffected by variations in the protein/lipid ratio. However, the fractional contribution of this component to the total enthalpy changes decreases with increases in peptide concentration, and this component completely disappears at higher protein mole fractions. The other component, which is less cooperative and occurs at a lower temperature, predominates at higher protein concentrations. These two components of the DSC endotherm have been assigned to the chain-melting phase transitions of peptide-nonassociated and peptide-associated PE molecules, respectively. Although the temperature at which the peptide-associated PE molecules melt is progressively decreased by increases in $(LA)_{12}$ concentration, the magnitude of this downward shift is progressively greater as the length of the PE hydrocarbon chain decreases. As well, mixtures of $(LA)_{12}$ with the longer chain PEs exhibit unusual biomodal enthalpy variations, suggesting peptide immiscibility in thicker gel state bilayers. Moreover, the enthalpy of the chain-melting transition of the peptide-associated PE does not decrease to zero even at high peptide concentrations, indicating that $(LA)_{12}$ attenuates but does not abolish the cooperative gel/liquid−crystalline phase transition of the lipids with which it is in contact. Our FTIR spectroscopic data indicate that $(LA)_{12}$ remains in a predominantly α-helical conformation in liquid−crystalline PE bilayers of various hydrophobic thickness but that the helical conformation is altered in gel-state PE bilayers generally, probably due to peptide lateral aggregation. These data also suggest that $(LA)_{12}$ significantly disorders the hydrocarbon chains of adjacent PE molecules in both the gel and liquid−crystalline states, relatively independently of lipid hydrocarbon chain length. Many aspects of PE/$(LA)_{12}$ interactions exhibit a different dependence on the hydrophobic thickness of the host bilayer than was observed in our previous study of $(LA)_{12}$-phosphatidylcholine (PC) model membranes [Zhang et al. (1995) *Biochemistry 34*, 2362−2371]. The differing effects of $(LA)_{12}$ incorporation on PE and PC bilayers is ascribed primarily to the much stronger lipid polar headgroup interactions characteristic of the former system. Finally, the considerable differences observed in the behavior of $(LA)_{12}$ and the related polyleucine-based peptide P_{24} in both PC and PE bilayers indicate that the structure of the hydrophobic core of α-helical transmembrane peptides can affect their conformational plasticity and state of aggregation and thus the nature of their interactions with different phospholipid bilayers.

The mutual interactions of lipids and proteins are fundamentally important to both the structure and the function of all biological membranes (*1*, *2*). In particular, the chemical composition and physical properties of the host lipid bilayer can markedly influence the activity and thermal stability of a large number of integral membrane proteins in both model and biological membrane systems (*1*−*5*). For this reason, there have been many studies of the interactions of membrane proteins with their host lipid bilayers, in both biological and reconstituted model membrane systems, employing a wide range of different physical techniques (*6*−*10*). However, our understanding of the physical principles underlying lipid−protein interactions remains incomplete and the actual molecular mechanisms whereby associated lipids actually alter the activity, and presumably also the structure and dynamics, of integral membrane proteins are largely unknown. This situation is due in part to the fact that most transmembrane proteins are relatively large, multidomain macromolecules of complex and often unknown three-

†This work was supported by operating and major equipment grants from the Canadian Institutes of Health Research and by a major equipment grant from the Alberta Heritage Foundation for Medical Research.

* To whom correspondence should be addressed. Telephone: 780-492-2413. Fax: 780-492-0095. E-mail: rmcelhan@gpu.srv.ualberta.ca.

10.1021/bi002170u CCC: $20.00
Published on Web 12/14/2000

dimensional structure and topology that can interact with lipid bilayers in complex, multifaceted ways (*1*−*10*). To overcome this problem, a number of workers have designed and synthesized peptide models of specific regions of natural membrane proteins and have studied their interactions with model lipid membranes of defined composition (*11*, *12*). Physical studies of such relatively tractable model membrane systems have already significantly advanced our understanding of the molecular basis of lipid−protein interactions.

The synthetic peptide acetyl-K_2−G−L_{24}−K_2−A-amide (P_{24})[1] and its analogues have been successfully utilized as a model of the hydrophobic transmembrane α-helical segments of integral membrane proteins (*12*, *13*). These peptides contain a long sequence of hydrophobic and strongly α-helical promoting leucine residues capped at both the N- and C-termini with two positively charged, relatively polar lysine residues. Moreover, the normally positively charged N-terminus and the negatively charged C-terminus have both been blocked to provide a symmetrical tetracationic peptide that will more faithfully mimic the transbilayer region of natural membrane proteins. The central polyleucine region of these peptides was designed to form a maximally stable α-helix, particularly in the hydrophobic environment of the lipid bilayer core, while the dilysine caps were designed to anchor the ends of these peptides to the polar surface of the lipid bilayer and to inhibit the lateral aggregation of these peptides. In fact, CD (*13*) and FTIR (*14*−*16*) spectroscopic studies of P_{24} have shown that it adopts a very stable α-helical conformation both in solution and in lipid bilayers, and X-ray diffraction (*17*), fluorescence quenching (*18*), and FTIR spectroscopic (*14*−*16*) studies have confirmed that P_{24} and its analogues assume a transbilayer orientation with the N- and C-termini exposed to the aqueous environment and the hydrophobic polyleucine core embedded in hydrocarbon core of the lipid bilayer when reconstituted with various PCs. DSC (*13*, *15*, *19*, *20*) and ^{2}H NMR spectroscopy (*13*, *19*, *20*) studies have shown that P_{24} broadens the gel/liquid−crystalline phase transition and reduces its enthalpy. The phase transition temperature is shifted either upward or downward, depending on the degree of mismatch between the hydrophobic length of the peptide and the hydrophobic thickness of PC lipid bilayers (*15*), but this is not observed in PE bilayers, where P_{24} substantially decreases the phase transition temperature in a hydrocarbon chain length-independent manner (*16*). As well, small distortions of the α-helical conformation of P_{24} are also observed in response to peptide−lipid hydrophobic mismatch (*15*). ^{2}H NMR (*22*) and ESR (*23*) spectroscopic studies have shown that the rotational diffusion of P_{24} about its long axis perpendicular to the membrane plane is rapid in the liquid-crystalline state of the bilayer and that a closely related peptide, acetyl-K_2−L_{24}−K_2-amide (L_{24}), exists at least primarily as a monomer in liquid−crystalline POPC bilayers, even at relatively high peptide concentrations.

A related peptide, $(LA)_{12}$, in which the polyleucine core of L_{24} is replaced by alternating leucine and alanine residues, has also been investigated to examine whether the replacement of one-half of the leucine residues by smaller and less hydrophobic alanine residues would influence the stability of the helical form of the peptide and if the surface topology of transmembrane peptides would affect their influence on lipid bilayers. The application of a variety of physical techniques has revealed that the behavior of $(LA)_{12}$ in solution and in lipid micelles or bilayers is generally similar to that of P_{24} (*24*, *25*). However, $(LA)_{12}$ perturbs the gel/liquid−crystalline phase transition of PC bilayers to a greater extent than does P_{24} at comparable concentrations, as inferred from the greater decrease of the temperature and enthalpy of the gel-to-liquid crystalline phase transition, possibly due partly to its rougher surface topology. However, the influence of the hydrophobic mismatch between the peptide and the host PC bilayer on the shift in the phase transition temperature is less pronounced for $(LA)_{12}$ than for L_{24}, perhaps due in part to the greater conformational plasticity of $(LA)_{12}$ in response to alterations of the bilayer thickness (*25*).

We report here the results of a DSC and FTIR spectroscopic study of the effect of the incorporation of $(LA)_{12}$ on the thermotropic phase behavior and organization of a homologous series of PE bilayers. The results of this study differ in many respects from those reported in our previous study of the same peptide incorporated into PC bilayers (*25*). As well, the behavior of P_{24} and $(LA)_{12}$ in both PC and PE model membrane systems also differ considerably. This and previous work thus demonstrate that the interactions between α-helical transmembrane peptides and lipid bilayers depend on the structure and physical properties of both the peptide and the host phospholipid bilayer.

MATERIALS AND METHODS

The phospholipids used in this study were either prepared in this laboratory (*26*) or obtained from Avanti Polar Lipids Inc. (Alabaster, AB). The peptide $(LA)_{12}$ was prepared as the hydrochloride salt using methods described Zhang et al. (*24*). Preparation of the lipid/peptide mixtures for DSC and FTIR spectroscopic studies proceeded as follows. Appropriate quantities of $(LA)_{12}$ and PE were codissolved in chloroform/methanol (1:2) to obtain the desired lipid/peptide ratio, and the solvent was removed in a stream of nitrogen at temperatures near 60−70 °C to ensure sample homogeneity (essential in the case of the longer chain PEs). Subsequently, the sample was dried in vacuo overnight. Typically, samples so prepared were subsequently hydrated and used as required. However, in cases in which more facile and convenient sample handling was required, the sample was redissolved in warm benzene and lyophylized to form a white powder. Our DSC studies showed that there were no differences between the thermotropic phase behavior of samples prepared by these two methods. For the DSC experiments, samples containing 0.8−2 mg of lipid were dispersed in 2 mL of water and hydrated by vigorous vortexing at temperatures 20−25 °C above the gel/liquid−crystalline phase transition temperature of the lipid. These samples were analyzed by a Microcal MC2 high-sensitivity differential scanning calorimeter (Microcal Inc., Amherst, MA) operating at heating rates between 10 and 30 °C per hour. Aside from the pure lipid, DSC thermograms were

[1] Abbreviations: P_{24}, acetyl-Lys_2−Gly−Leu_{24}-Lys_2−Ala-amide; L_{24}, acetyl-Lys_2−Leu_{24}−Lys_2-amide; $(LA)_{12}$, acetyl-Lys_2−$(Leu-Ala)_{12}$−Lys_2-amide; PE, phosphatidylethanolamine; PC phosphatidylcholine; DSC, differential scanning calorimetry; FTIR, Fourier transform infrared spectroscopy; CH_2, methylene. The hydrocarbon chain lengths of the lipids used in this study are described by the shorthand notation *N*:0 with *N* representing the number of carbon atoms in the chain and 0 indicating the absence of carbon−carbon double bonds.

Table 1: Hydrophobic Thicknesses of the Bilayers Formed by Various Phosphatidylethanolamines[a]

PE	hydrophobic thickness (Å)[a]		
	gel phase	liquid−crystalline phase	mean[b]
11:0	26.9	18.1	22.5
12:0	29.3	19.7	24.5
13:0	31.8	21.3	26.5
14:0	34.2	22.8	28.5
16:0	39.4	26.3	32.9
18:0	44.7	29.8	37.3
20:0	48.8	32.8	40.8

[a] Hydrophobic thicknesses were estimated using the equations developed by Sperotto and Mouritsen (1988) to calculate the hydrophobic thicknesses of PC bilayers. [b] The mean of the hydrophobic thicknesses of the gel and liquid−crystalline phases.

recorded with lipid/peptide mixtures with mole percents of peptides ranging from 1.0 to 10.0 (i.e., lipid/peptide ratios of 100:1 to 10:1). The data obtained were analyzed and plotted with the Origin program supplied by Microcal Software Inc. (Northampton, MA). For the FTIR spectroscopic experiments, 2−3 mg samples were hydrated with 75 μL of D_2O by vigorous vortexing under the same conditions described above. This produced a paste that was squeezed between two BaF2 windows of a demountable liquid cell that was equipped with a 25 μM Teflon spacer. After reassembly, the cell was placed in a holder where its temperature could be regulated between −20 and 90 °C by means of an external computer-controlled circulating water bath. FTIR spectra were recorded with a Digilab FTS-40 Fourier transform instrument (Digilab Inc., Cambridge, MA) using data acquisition and data processing parameters similar to those described by Mantsch et al. (*27*). Data were analyzed with the aid of software supplied by Digilab Inc. and other computer programs available from the National Research Council of Canada. To assist in the interpretation of some of the complex, multicomponent bands observed, Fourier deconvolution methods were used to obtain estimates of the band frequencies. These estimates were then used in curve fitting to the original spectra to obtain estimates of the width and integrated intensities of the band components. Typically, Fourier deconvolution was employed with band narrowing factors of 1.8−2.0 and curve fitting was performed with a Gaussian/Lorentzian function with a 70% Gaussian fraction.

RESULTS

Differential Scanning Calorimetry. In considering the DSC and FTIR spectroscopic data presented below, it is important to compare the intrinsic hydrophobic length of the $(LA)_{12}$ peptide with the intrinsic hydrophobic thicknesses of the various PE bilayers used in this study. On the basis of measurements of a molecular model of this peptide in which its entire leucine−alanine core adopts an ideal α-helical conformation, we estimate that the mean hydrophobic length of $(LA)_{12}$ (the average length of the leucine−alanine sequence measured at any point on the surface of the helix) is 30.6 Å (*15*). Given this value and the calculated hydrophobic thicknesses of the various PE bilayers in their gel and liquid-crystalline states (see Table 1), the following points should be noted. In the gel phase, the hydrophobic length of $(LA)_{12}$ will exceed the hydrophobic thickness of 11:0 and 12:0 PE bilayers but will be progressively less than the hydrophobic thicknesses of the longer chain PE bilayers. In the liquid−crystalline phase, $(LA)_{12}$ hydrophobic length will progressively exceed the hydrophobic thickness of all PEs with hydrocarbon chains of 18 or fewer carbon atoms but will be less than the hydrophobic thickness of the 20:0 PE bilayer. Thus for the shorter chain 11:0 and 12:0 PE bilayers, $(LA)_{12}$ hydrophobic length exceeds phospholipid bilayer thickness in both the gel and the liquid−crystalline phases, while $(LA)_{12}$ hydrophobic length is always less than bilayer thickness for 20:0 PE. For the intermediate chain length PEs (13:0−18:0 PE), the hydrophobic length of $(LA)_{12}$ will be less than that of gel state but more than that of the liquid−crystalline bilayer, with the best match of peptide and PE mean hydrophobic lengths occurring for the 14:0 and 16:0 PE bilayer systems.

We stress here that the pattern of matching of lipid bilayer thickness and peptide hydrophobic length just described applies only if $(LA)_{12}$ adopts an ideal α-helical conformation that is not influenced by lipid bilayer thickness. However, our previous calorimetric and spectroscopic studies of the polyleucine-based peptide P_{24} suggest that even this relatively conformationally rigid, strongly α-helical peptide can alter the pitch of its helix slightly in response to variations in host bilayer thickness (*15*, *21*). Moreover, our previous studies of $(LA)_{12}$ indicate that this peptide is less strongly α-helical and more conformationally responsive to changes in the physical properties of its host PC bilayer than is P_{24} (*24*, *25*). As well, in thick gel state PC bilayers, $(LA)_{12}$ (but not P_{24}) cannot only vary the pitch of its α-helix but can also form a mixture of α-helical and other helical forms (*25*). Conversely, the hydrocarbon chains of PC and PE bilayers can also change their degree of conformational order, and thus their effective hydrophobic thickness, to accommodate to the presence of these model peptides (*15*, *21*, *25*). Thus the actual degree of hydrophobic mismatch between $(LA)_{12}$ and the various PE bilayers, in both the gel and the liquid−crystalline states, may be less than indicated from the intrinsic hydrophobic length of this peptide and from the data presented in Table 1, which is for PE bilayers in the absence of peptide.

Thermotropic Phase Behavior of the Pure Phosphatidylethanolamines. As illustrated in Figure 1, unannealed aqueous dispersions of all the PEs studied here undergo a single fairly energetic and highly cooperative phase transition upon heating. This transition, which is completely reversible, arises from a conversion of the lamellar gel to the lamellar liquid−crystalline state. As expected, the temperature and enthalpy of these chain-melting phase transitions increase progressively with increases in hydrocarbon chain length. For a thorough discussion of the thermotropic phase behavior of the complete homologous series of linear diacyl PEs, the reader is referred to Lewis and McElhaney (*26*) and references therein.

Thermotropic Phase Behavior of Peptide/Phosphatidylethanolamine Mixtures. Also illustrated in Figure 1 are DSC heating scans of various PE vesicles containing low, intermediate, and high concentrations of $(LA)_{12}$. Despite the large variation in bilayer thickness relative to $(LA)_{12}$ intrinsic hydrophobic length, the overall thermotropic phase behavior of all of the peptide-containing PE bilayers studied is generally similar, depending primarily on the lipid/peptide ratio of the vesicle and only secondarily on the length of

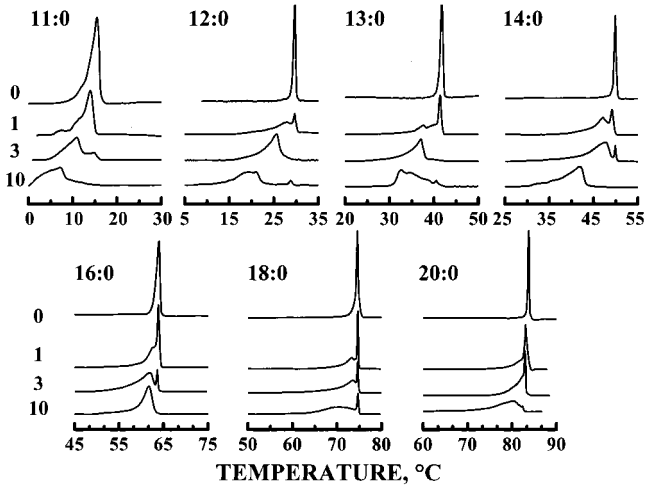

FIGURE 1: DSC heating thermograms of aqueous dispersions of the *n*-saturated 1,2-diacyl PEs and their mixtures with the peptide $(LA)_{12}$. The mol % peptide present in the PE vesicles is indicated on the left side of this figure.

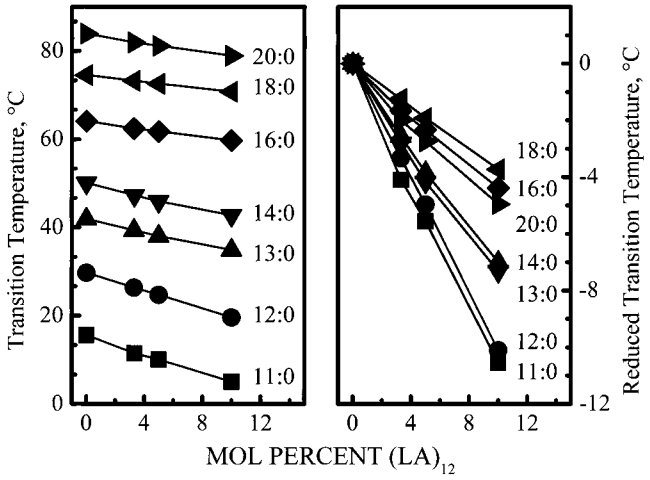

FIGURE 2: Effect of $(LA)_{12}$ content on the gel to liquid−crystalline phase transition temperature of the PE/$(LA)_{12}$ mixtures. Data are presented for the broad components of the DSC endotherms obtained with mixtures of peptide and PEs of the hydrocarbon chain lengths indicated. The left panel shows the plots of absolute transition temperature as a function of peptide concentration in mol percent and the right panel shows plots of the observed transition temperature relative to that of the pure lipid.

the phospholipid hydrocarbon chains (see below). Specifically, at lower levels of incorporated peptide, the DSC traces clearly consist of two components, a lower temperature, less cooperative endotherm and a higher temperature, more cooperative endotherm. The relative contribution of the sharper component, which initially exhibits phase transition thermodynamic parameters almost identical to those of the pure phospholipid, progressively decreases as the amount of peptide incorporated increases, and this component disappears entirely when peptide concentration approaches 5 mol %. In contrast, the relative contribution of the broader component increases with increases in peptide concentration, and this component is the only one that persists at the higher levels of peptide incorporation. Moreover, our FTIR spectroscopic studies (see below) indicate that both endotherms arise from the melting of the hydrocarbon chains of the host PE bilayer. We thus assign the sharp component of these DSC traces to the gel/liquid−crystalline phase transition of peptide-poor PE domains and the broad component to the chain melting of peptide-rich PE domains, as in our previous studies of the interactions of P_{24} with PC (*15*) and PE (*21*) bilayers and of $(LA)_{12}$ with PC bilayers (*25*). Finally, we note that the overall thermotropic phase behavior of the P_{24}-containing PE bilayers studied previously (*21*) and of the $(LA)_{12}$-containing PE bilayers studied here are generally similar except for the shortest and longest chain PEs examined. Specifically, we found previously that the presence of small quantities of P_{24} accelerate the formation of the lamellar crystalline phase of short chain PE bilayers and that larger quantities of P_{24} undergo a time and scan number-dependent demixing in 20:0 PE bilayers. However, neither of these phenomenon were noted in the present study of $(LA)_{12}$-containing PE bilayers, where repeated heating and cooling through the regions of the phospholipid phase transitions produce no changes in these DSC thermograms.

The effects of the incorporation of increasing quantities of $(LA)_{12}$ on the temperatures of the sharp and broad components of the DSC endotherms are quite different and exhibit a different dependence of the hydrocarbon chain length of the host PE bilayer. The presence of increasing quantities of peptide results in only a very slight decrease in the temperature of the sharp component and the magnitude of this decrease is essentially independent of PE hydrocarbon chain length (see Figure 1). Such an effect has also been noted in all of our previous studies of transmembrane peptide−phospholipid interactions and has been ascribed to the slight destabilization of the peptide-free gel state domains of the phospholipid bilayer by the presence of protein at the edges of such domains (*15*, *21*, *25*). In contrast, increasing levels of peptide progressively lower the temperature of the broad component of the DSC thermogram but in a hydrocarbon chain-length dependent manner (see Figure 2). Specifically, the presence of a given quantity of peptide reduces the chain-melting phase transition temperature of the shorter chain PE bilayers to a much greater extent than for the longer chain bilayers. Interestingly, the reduction of the temperature of the broad phase transition of the PE bilayers by the polyleucine-based peptide P_{24} is independent of PE bilayer thickness and, except for the longest chain PEs studied, is smaller in magnitude than for comparable levels of $(LA)_{12}$ (*21*). This result suggests that $(LA)_{12}$ is more disruptive to the organization of gel state PE bilayers than is P_{24}. The possible molecular basis for this difference in the effects of these two peptides on the stability of gel state PE bilayers will be examined in the Discussion.

The $(LA)_{12}$-induced changes in the enthalpy of the hydrocarbon chain-melting phase transitions of the *n*-saturated 1,2-diacyl PE vesicles studied here are summarized in Figure 3. The values plotted therein are derived from the combined areas of the broad and narrow components of the DSC thermograms recorded. With all of the PEs studied, the incorporation of low levels of $(LA)_{12}$ results in a progressive decrease in the measured transition enthalpy whether viewed on the absolute or relative scale. Moreover, with the shorter chain PEs, progressive decreases in the enthalpy are observed over the entire range of protein concentrations examined. However, as PE hydrocarbon chain length increases, further increases in $(LA)_{12}$ content result in progressively smaller decreases in the measured enthalpy and with the longer chain PEs, further increases in peptide incorporation actually cause an apparent increase in the

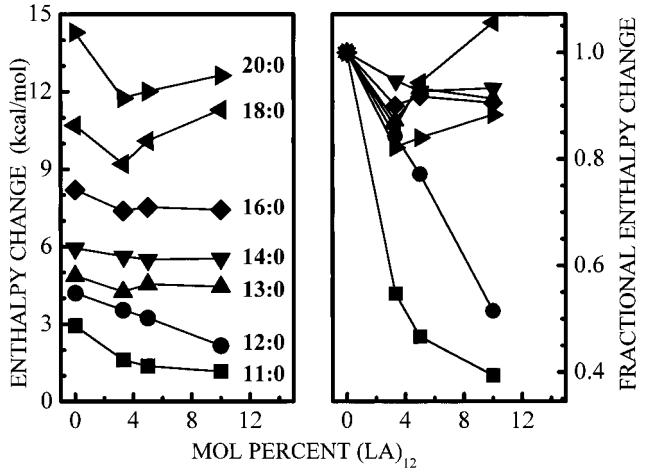

FIGURE 3: Effect of $(LA)_{12}$ content on the apparent total enthalpy of the hydrocarbon chain-melting phase transition of PE/$(LA)_{12}$ mixtures. Data are presented as a function of peptide mol % for mixtures containing PEs of the hydrocarbon chain lengths indicated.

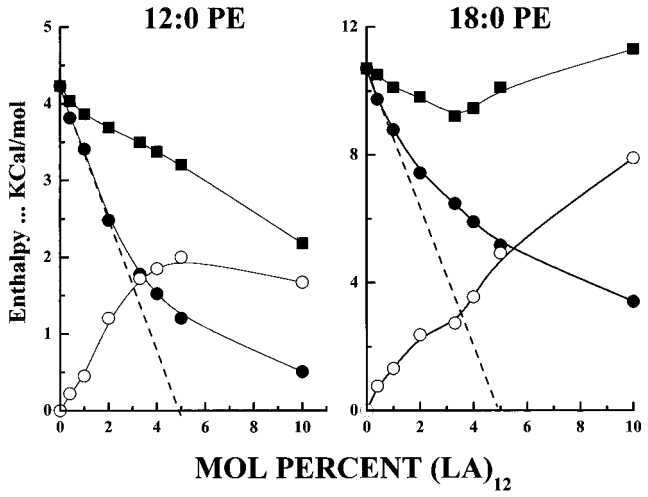

FIGURE 4: Effect of peptide content on the total enthalpy of the gel/liquid−crystalline phase transition (-■−■-) and on the sharp (-●-●-) and broad (-○−○-) components of the DSC endotherms of $(LA)_{12}$-containing PE liposomes. Data are presented for liposomes composed of 12:0 PE and 18:0 PE to illustrate the patterns exhibited by lipid/peptide mixtures derived from the short and long chain PEs. Extrapolation of the initial linear portion of the sharp component enthalpy values is illustrated by the dashed line.

measured enthalpy values. A similar phenomenon was noted in our previous studies of P_{24}-containing PE bilayers and was attributed to contributions from the "heat of dispersal" of the peptide, which is laterally aggregated at low temperatures, in the more disordered lipid domains that form at temperatures near the phase transition temperature (*21*). The qualitative similarity between this particular aspect of our data and our previous studies of P_{24}-containing PE bilayers suggests that a similar process may be occurring when high levels of $(LA)_{12}$ are incorporated into the longer chain PE systems. This possibility will be explored more fully in the Discussion. Note, however, that even in the absence of this phenomenon, as in the shorter chain PEs, the total enthalpy of the chain-melting phase transition does not approach zero, even at the highest peptide concentration tested, indicating that this peptide can reduce the enthalpy and cooperativity of the gel/liquid−crystalline phase transition but not abolish it entirely.

The enthalpy values for the sharp and broad components of the DSC thermograms of 12:0 PE and 18:0 PE vesicles containing various quantities of $(LA)_{12}$ are illustrated in Figure 4. In both cases, the enthalpy of the sharp component decreases markedly with increases in peptide concentration and approaches zero as the peptide concentration increases to 10 mol %. Similarly, the enthalpy of the broad component increases markedly and is responsible for essentially all of the total enthalpy at the higher peptide concentrations. If one assumes that the sharp component of the DSC endotherm represents the chain melting of essentially pure PE domains, then the dependence of the enthalpy of this component on peptide concentration should reflect the stoichiometry of peptide/lipid interactions (*6*). Extrapolation of the initial slope of the enthalpy of the sharp component of the DSC endotherm versus peptide concentration to zero enthalpy results in an X intercept value of about 5 mol % peptide, indicating that each $(LA)_{12}$ molecule interacts directly with, and perturbs the phase behavior of, about 20 PE molecules. This value is similar to that determined in our earlier studies of P_{24}-containing PC (*15*) and PE (*21*) bilayers and of $(LA)_{12}$-containing PC bilayers (*25*). Moreover, these values are in good agreement with an earlier study in which model building was used to estimate that about 16−18 molecules of phospholipid would be required to form a single boundary or solvation layer around each P_{24} molecule in the gel state (*20*). However, at higher peptide concentrations, this plot becomes curved and the transition enthalpy of the sharp component of the DSC endotherm does not approach zero until $(LA)_{12}$ concentrations near 10 mol % are reached. This latter observation was also noted in our previous study of $(LA)_{12}$/PC bilayer systems (*25)* but not in our studies of mixtures of P_{24} with PC or PE bilayers, where similar plots exhibit much less curvature such that the enthalpy approaches zero at much lower peptide concentrations (*15*, *21*). These results imply that $(LA)_{12}$ (but not P_{24}) molecules are aggregated within the bilayer at higher peptide concentrations in gel state bilayers, since a significant degree of lateral clustering would replace lipid−protein with protein−protein contacts and thus reduce the apparent lipid−protein stoichiometry observed by DSC (*6*).

The effect of the incorporation of $(LA)_{12}$ on the cooperativity of the broad component of the DSC thermograms of various PE vesicles is illustrated in Figure 5. In general, the widths of the broad component endotherms exhibit only a weak dependence on the amount of peptide present and on the hydrocarbon chain length of the host PE bilayer. Similar results were reported previously for the polyleucine-based peptide P_{24} in a homologous series of PE bilayers (*21*). However, at comparable peptide concentrations, the width of the gel and liquid-crystalline phase coexistence regions is greater in PE bilayers containing $(LA)_{12}$ than in the same bilayers containing P_{24}.

Fourier Transform Infrared Spectroscopy. In these studies, FTIR spectra of various $(LA)_{12}$-containing PE vesicles were recorded as a function of temperature and as a function of peptide concentration. FTIR spectroscopy provides a nonperturbing method of monitoring both the structural organization of the host lipid bilayer and the conformation of the incorporated peptide. In particular, the phase state and orientational order of the PE hydrocarbon chains can be conveniently determined by measuring the frequency and

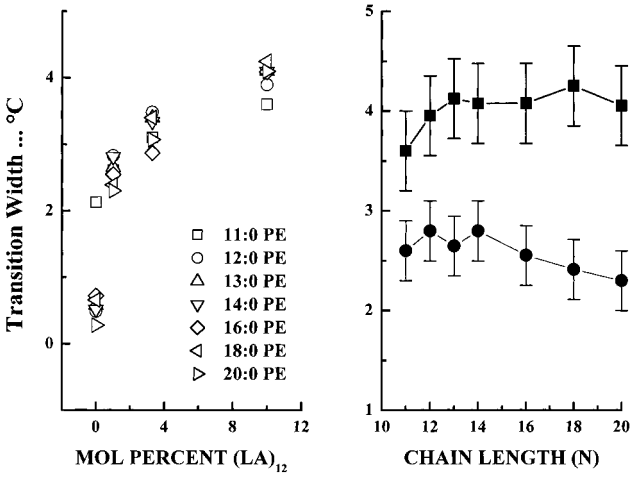

FIGURE 5: Plots of the transition width in °C of the broad components of the DSC endotherm versus the mol % of $(LA)_{12}$ (left panel) or versus the hydrocarbon chain length of the host PE bilayer (right panel), at peptide concentrations of 3.3 (-●-●-) and 10 (-■−■-) mol %, respectively. To minimize the contribution of the anomalous broad endothermic component observed at higher peptide concentrations in the longer chain PEs (see text), the transition widths were measured from the temperatures of 25 to 75% conversion from the gel to the liquid−crystalline state.

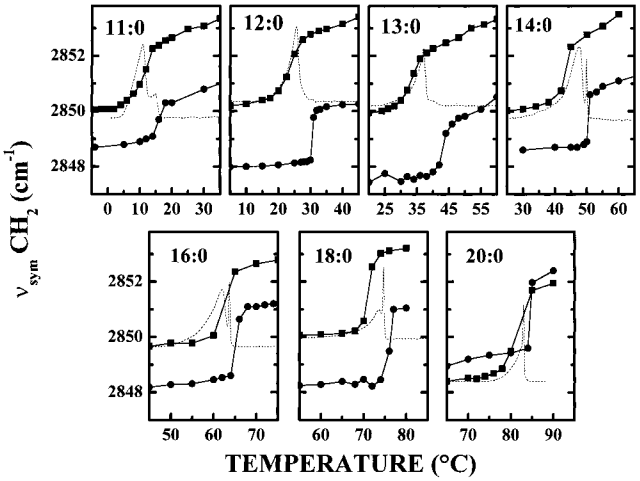

FIGURE 6: Effect of temperature on the frequencies of the CH_2 symmetric stretching bands of pure PE bilayers and of their mixtures with the peptide $(LA)_{12}$. Data are shown for PEs of the hydrocarbon chain lengths indicated. The circles represent data obtained with the pure lipids and the squares represent data obtained with PE/$(LA)_{12}$ mixtures containing 3.3 mol % peptide (a lipid/peptide molar ratio of 30:1). To facilitate comparison between these FTIR spectroscopic data and the DSC results, DSC thermograms of the lipid/peptide mixtures (- - -) are superimposed on the same temperature scale.

bandwidth of the CH_2 symmetric stretching band near 2850 cm^{-1}, and the conformation of the peptide can be monitored by measuring the frequency of the amide I band near 1650 cm^{-1} (see ref *28* for reviews).

We present below FTIR spectroscopic data from various PE vesicles having a peptide mole percent of 3.3 (30 PE molecules per molecule of peptide). This moderate concentration of $(LA)_{12}$ was chosen to provide sufficient peptide to accurately monitor its conformation while also ensuring that sufficient lipid was present to fully solvate each peptide molecule, thus minimizing the potential for peptide−peptide contacts and possible lateral aggregation within the host lipid bilayer. DSC endotherms of the PE/peptide mixtures are also included in the figures presented below to facilitate comparison of the calorimetric and spectroscopic results. The temperature-dependent changes in the frequency of CH_2 symmetric stretching bands of pure PEs and of their mixtures with $(LA)_{12}$ are illustrated in Figure 6. Upon heating the pure lipids, the CH_2 symmetric stretching bands exhibit a discontinuous increase in frequency of 2.0−2.5 cm^{-1} at temperatures that coincide with the energetic and highly cooperative heating endothermic transition observed in the DSC experiment. This increase in frequency is also accompanied by a discontinuous increase in the width of the CH_2 symmetric stretching band (data not shown). Together, these changes are characteristic of phospholipid hydrocarbon chain-melting phase transitions and arise from the increase in hydrocarbon chain mobility and conformational disorder that occur when all-trans polymethylene chains melt (see ref *28* and references therein). Figure 6 also shows that comparable increases in the frequencies of the CH_2 symmetric stretching bands are also observed upon heating aqueous dispersions of the PE/peptide mixtures. However, these frequency increases occur over a broader temperature range than observed with the pure lipids and also occur over the same temperature range as do the corresponding DSC heating endotherms. This observation clearly indicates that both the sharp and the broad components of the DSC endotherms result from the melting of the hydrocarbon chains of the host lipid bilayer. However, as shown in Figure 6, the CH_2 symmetric stretching frequencies exhibited by the lipid mixtures are higher both above and below the phase transition temperature than those of the pure PEs in all cases except for the 20:0 PE mixture. Since the frequency of the CH_2 symmetric stretching band is roughly correlated with the overall degree of hydrocarbon chain conformational disorder (*28*), these results suggest that the presence of $(LA)_{12}$ produces a decrease in the conformational order of the hydrocarbon chains of the host PE bilayer in both the gel and the liquid−crystalline states. Very similar results were observed in our previous studies of P_{24}-containing PE bilayers (*21*). The markedly reduced effect of the incorporation of $(LA)_{12}$ on the conformational order of the hydrocarbon chains of the 20:0 PE bilayer may be due to its limited miscibility in this thick bilayer system, although such a limited miscibility was not obvious in our calorimetric analysis of the thermotropic phase behavior of this mixture. Again, a similar effect was noted previously in P_{24}-containing 18:0 and 20:0 PE vesicles (*21*).

The conformational sensitivity of $(LA)_{12}$ to changes in the physical properties of its host PE matrix was evaluated by an examination of the contours of the peptide amide I absorption band as a function of temperature, as illustrated in Figure 7. Previous work has shown that $(LA)_{12}$ adopts a predominantly α-helical conformation under all conditions examined so far (*24*, *25*) and, consistent with this, the dominant feature of its amide I absorption band of this peptide in various media is a sharp component centered near 1655 cm^{-1}. The data shown in Figure 7 illustrate that this feature is also retained when $(LA)_{12}$ is incorporated into 12:0 bilayers in both the gel and the liquid−crystalline states. Similar results were obtained for other short, medium, and long chain PEs (data not presented). However, the contours of the peptide amide I absorption band are also affected by the phase state of its host lipid. Specifically, in the liquid−

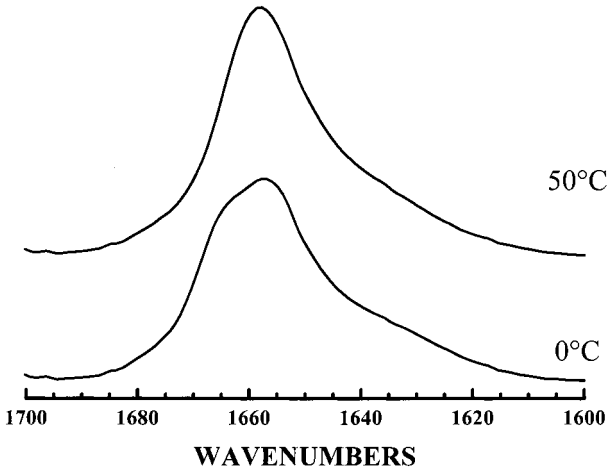

FIGURE 7: FTIR spectra showing the contours of the amide I absorption bands of $(LA)_{12}$ dispersed in 12:0 PE bilayers at a peptide concentration of 3.3 mol % (a lipid/peptide ratio of 30:1). The absorbance spectra shown were acquired in the gel (0 °C) and liquid−crystalline states (50 °C) of this lipid/peptide mixture.

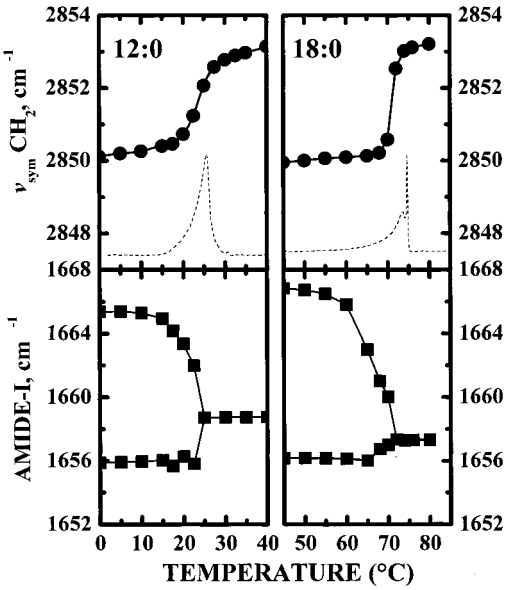

FIGURE 8: Temperature dependence of the components of the amide I absorption bands of $(LA)_{12}$ in a PE bilayer matrix (—■—) containing 3.3 mol % peptide. The frequencies of the amide I absorption band components are plotted as a function of temperature in the bottom panels of the Figure. Data acquired with the 12:0 PE-based mixture are shown in the left panel and those obtained with the 18:0 PE-based mixture are shown on the right. To better illustrate the correspondence between temperature-dependent changes in the peptide amide I band and the thermotropic phases behavior of the lipid/peptide mixture, the DSC thermograms (- - -) and the temperature dependent changes in the lipid CH_2 symmetric stretching bands (—●—) are plotted on the same temperature scale in the top panels.

crystalline phases of all PE/$(LA)_{12}$ mixtures examined, the amide I absorption between 1650 and 1670 cm^{-1} consists of a single component centered near 1655 cm^{-1}, whereas in the gel phases this absorption band is split into components centered near 1655 and 1665 cm^{-1}. Moreover, this additional higher-frequency component is observed in the gel states of mixtures derived from PEs with short, medium, and long hydrocarbon chains. Also, as illustrated in Figure 8, this particular component begins to disappear from the infrared spectrum at temperatures that coincide with the onset of the broad component observed by DSC and with the onset of hydrocarbon chain melting as detected by FTIR spectroscopy. Interestingly, this component of the amide I absorption band of $(LA)_{12}$ has also been observed in the gel phases of $(LA)_{12}$-containing PC bilayers (*25*). However, this higher frequency component of the amide I band has only been observed in the gel phases of mixtures derived from the PCs with hydrocarbon chain lengths of at least 18 carbon atoms. The possible molecular basis of this observation will be examined further in the Discussion.

DISCUSSION

There are both similarities and differences in the thermotropic phase behavior of $(LA)_{12}$-containing PC (*25*) and PE model membranes. In both phospholipids, the incorporation of relatively low concentrations of this peptide generally produces two-component DSC endotherms consisting of a more cooperative, higher temperature component and a less cooperative, lower temperature component. Moreover, the temperature and cooperativity of the former component is relatively insensitive to peptide concentration and closely resembles the DSC endotherm of the pure lipid, whereas the temperature and cooperativity of the latter component are much more sensitive to peptide concentration in both cases. Moreover, the relative contribution of the sharp component to the total enthalpy of the phospholipid gel/liquid−crystalline phase transition decreases continuously with increasing peptide concentration, vanishing entirely at high concentrations, whereas the relative enthalpic contribution of the broad component initially increases with increasing peptide concentration. Thus in both PC and PE bilayers, lower concentrations of $(LA)_{12}$ appear to induce the formation of peptide-poor and peptide-rich phospholipid domains, respectively, until the peptide concentration exceeds a certain value, in which case pure lipid domains can no longer be detected calorimetrically. As well, based on the dependence of the transition enthalpy of the sharp component on peptide concentration, in both systems each molecule of $(LA)_{12}$ appears to interact with about 20 phospholipid molecules at low peptide concentrations, but at higher peptide concentrations lateral aggregation of $(LA)_{12}$ in gel-state bilayers appears to occur. Thus, in terms of their overall thermotropic phase behavior, $(LA)_{12}$ seems to have broadly similar effects on both PC and PE bilayers.

There are, however, also some significant quantitative and even qualitative differences between the effects of $(LA)_{12}$ incorporation on specific aspects of the thermotropic phase behavior of PC and PE bilayers. For example, the addition of increasing quantities of $(LA)_{12}$ to PC bilayers results in a small (1−2 °C) upward shift in the temperature of the broad component of the DSC endotherm relative to that of the sharp component, and this upward shift appears to be almost independent of hydrocarbon chain length (*25*). These results indicate that $(LA)_{12}$ incorporation has only a small effect on the relative stability of the gel and liquid−crystalline states of PC bilayers and that the effects of any mismatch between the hydrophobic length of the peptide and the hydrophobic thickness of the host lipid bilayer are markedly attenuated in this system. In contrast, the addition of increasing quantities of $(LA)_{12}$ to PE bilayers produces a more marked downward shift in the temperature of the broad component of the DSC endotherm relative to that of the sharp component. Moreover, although this reduction in temperature is

relatively independent of hydrocarbon chain length in the longer chain PEs (16:0−20:0 PE), the magnitude of this reduction increases markedly as hydrocarbon chain length decreases in the shorter chain PEs (12:0−14:0 PE). However, since the hydrophobic length of the peptide should match the hydrophobic thickness of the host gel state PE bilayer fairly well for the shorter chain PEs but should appreciably exceed the hydrophobic thickness of these shorter chain PE bilayers in the liquid-crystalline state (see Table 1), hydrophobic mismatch theory predicts that the incorporation of this peptide should differentially stabilize the gel relative to the liquid−crystalline state, thereby increasing rather than decreasing the chain-melting phase transition temperature of the shorter chain PEs. Clearly, then, hydrophobic mismatch effects per se cannot explain our experimental results.

We note that somewhat similar general results were obtained in our previous comparative studies of the effect of the structurally related α-helical transmembrane peptide P_{24} on PC (*15*) and PE (*21*) bilayers. These studies revealed that P_{24} incorporation significantly increases the gel/liquid−crystalline phase transition temperature of PC bilayers as hydrocarbon chain length is reduced and less significantly decreases this temperature as hydrocarbon chain length was increased. In contrast, P_{24} incorporation into PE bilayers results in a progressive and more significant reduction in the gel/liquid−crystalline phase transition temperature independent of hydrocarbon chain length. We rationalized these previous results by postulating that relatively strong electrostatic and hydrogen-bonding headgroup−headgroup interactions contribute significantly to the stabilization of PE bilayers, whereas such interactions are much weaker in PC bilayers (*26*, *29*−*32*). Thus, at the surfaces of hydrated PE bilayers, the phosphoryl ethanolamine headgroups probably form part of a dynamic network of intermolecular electrostatic and hydrogen-bonding interactions involving the amino and phosphate moieties of the headgroups as well as the surrounding water molecules. We therefore suggested that the observed decrease in phase transition temperature coincident with the introduction of P_{24} into PE bilayers can be directly attributed to its disruption of the hydrogen-bonding network, because the access of any PE molecule to potential hydrogen-bonding partners is substantially reduced by its proximity to and contact with the peptide. Most probably this effect is a function of peptide concentration and, given the importance of the integrity of the hydrogen-bonding network to the stability of PE bilayers, it may be large enough to effectively mask effects attributable to the mismatch of peptide hydrophobic length and bilayer hydrophobic thickness. It is also possible that the positively charged lysine residues on the ends of the peptide may locally disrupt the attractive electrostatic interactions between adjacent PE molecules in the bilayers. Although the explanation provided above can successfully rationalize both the generally more disruptive effect of $(LA)_{12}$ incorporation on PC than on PE bilayers and the lack of an effect of hydrocarbon chain length variation in the longer chain PEs, it does not provide an explanation for the greater effect of $(LA)_{12}$ incorporation on the phase transition temperature of the shorter than on the longer chain PEs. However, this observation, and the bimodal effect of $(LA)_{12}$ incorporation on the apparent enthalpy of the gel/liquid phase transition observed here and in a previous study of P_{24}/PE mixtures (*21*), may be rationalized by postulating a hydrophobic mismatch effect on the lateral miscibility of $(LA)_{12}$ in gel state PE bilayers. In this regard, we note that in the shorter chain PE bilayers, where the match of peptide hydrophobic length and bilayer hydrophobic thickness is good, the enthalpy of the gel/liquid−crystalline phase transition decreases progressively with increases in $(LA)_{12}$ concentration, as expected from the disordering effect of incorporated transmembrane peptides on phospholipid hydrocarbon chains in the gel state (*6*). However, as peptide hydrophobic length becomes increasingly smaller than gel state bilayer thickness in the longer chain PEs, the apparent reduction in the enthalpy of the chain-melting phase transition becomes increasingly attenuated and eventually actually appears to increase at higher peptide concentrations. We note, however, that the DSC endotherms of the longer chain PE/$(LA)_{12}$ mixtures appear to consist of a higher temperature, more cooperative component superimposed over a much less cooperative, lower temperature component, the latter manifesting as an upward curvature of the baseline in the temperature region beginning at temperatures below but extending into the temperature region of the more cooperative endotherm. Since our FTIR results indicate that the lower temperature, less cooperative endotherm is not a hydrocarbon chain-melting process while the more cooperative endotherm is, we propose that $(LA)_{12}$ has an increasingly limited lateral miscibility in longer chain PE bilayers at low temperatures. Thus, we suggest that the additional less cooperative, lower temperature component observed calorimetrically at higher peptide concentration results from the heat absorbed by the "dissolution" of laterally aggregated peptide present in the thicker, highly ordered gel state bilayer domains into the thinner, more disordered liquid−crystalline domains that form as the temperature approaches the chain-melting phase transition temperature of the host lipid bilayer. Since this dissolution process would be expected to become quantitatively more important both with increases in peptide concentration and increases in PE hydrocarbon chain length, it accords well with our experimental observations. This hypothesis would also explain why the presence of $(LA)_{12}$ reduces the phase transition temperature of the shorter chain PEs to a greater extent than of the longer chain PEs, since the number of peptide−lipid contacts would be limited in the thicker gel state bilayer formed by these latter phospholipids due to the lateral aggregation of the peptide inclusions. Support for this hypothesis is also provided by a recent study of the structurally related WALP and KALP α-helical transmembrane peptides, which indicate that these peptides can form laterally aggregated striated domains in gel state PC bilayers (*33*).

Another example of the difference in the behavior of PC and PE bilayers containing $(LA)_{12}$ relates to the apparently different conformations of the peptide in gel state bilayers of different hydrophobic thickness. When incorporated into shorter chain PC bilayers, a single predominant peptide amide I band centered near 1657 cm^{-1} is observed by FTIR spectroscopy in the liquid−crystalline state, and the frequency of this band increases only slightly ($\sim$1 cm^{-1}) in the gel state. This behavior is compatible with $(LA)_{12}$ existing exclusively in the α-helical conformation in both solid and fluid PC bilayers, with perhaps a small alteration in helical pitch in the thicker gel state systems (*25*). However, in the

longer chain PCs, the major amide I band of $(LA)_{12}$ splits into a doublet with maxima near 1656 and 1667 cm^{-1} when the PC bilayer enters the gel state. We have interpreted this result to indicate that a portion of the $(LA)_{12}$ molecules have undergone a conformational alteration induced by a hydrophobic mismatch between the peptide and the much thicker gel state bilayers formed by the longer chain PCs. Alternatively, this large change in the spectroscopic behavior of $(LA)_{12}$ in long chain PC gel state bilayers could be due to peptide conformation changes resulting from the lateral aggregation of peptide molecules in the longer chain PC systems (*25*). In contrast, the present study shows that this splitting of the peptide amide I band of $(LA)_{12}$ into two components in the gel state occurs in bilayers composed of short and medium chain, as well as long chain, PEs. Thus, in PE bilayers, amide I band splitting depends only on phospholipid phase state but not on the hydrophobic thickness of the gel state bilayer, in contrast to PC bilayers.

Again, this difference in spectroscopic behavior could be rationalized by postulating that $(LA)_{12}$ molecules have a greater lateral miscibility in PC as compared to PE bilayers, as indeed appears also to be the case for the structurally related peptide P_{24} (*15*, *21*). However, the splitting of the amide I band of P_{24} is not observed in gel state PC or PE bilayers, even those generated from long chain phospholipids (*15*, *21*). This finding would in turn suggest that P_{24} exhibits a generally higher degree of lateral miscibility in phospholipid bilayers than does $(LA)_{12}$. Indeed, such behavior might be expected based on the topologically smoother and more hydrophobic surface of P_{24} and compared to $(LA)_{12}$.

In conclusion, the results of this and a number of previous studies clearly show that lipid−peptide interactions are sensitive to relatively small alterations in the chemical structure and physical properties of both the peptide and the host lipid bilayer. In many cases, the subtlety and complexity of these interactions are not readily predicted or rationalized by current theoretical models. This result indicates that considerable additional experimental and theoretical work will be required to elucidate the molecular basis for the interesting and potentially biologically relevant phenomenon that are exhibited by these relatively "simple" peptide−lipid model membrane systems.

REFERENCES

1. Gennis, R. B. (1989) *Biomembranes: Molecular Structure and Function*, Springer-Verlag, New York.
2. Yeagle, P. (1992) *The Structure of Biological Membranes*, CRC Press, Boca Raton, FL.
3. Sandermann, H. (1978) *Biochim. Biophys. Acta 515*, 209−237.
4. McElhaney, R. N. (1982) in *Current Topics in Membranes and Transport* (Razin, S., and Rottem, S., Eds.) Vol. 17, pp 317−380, Academic Press, New York.
5. McElhaney, R. N. (1985) in *Membrane Fluidity in Biology* (Aloia, R. A., and Boggs, J. M., Eds.) Vol. 4, pp 147−208, Academic Press, New York.
6. McElhaney, R. N. (1986) *Biochim. Biophys Acta 864*, 361−421.
7. Watts, A., and De Pont, J. J. H. H. M., Ed. (1985) *Progress in Lipid−Protein Interactions*, Vol. 1, Elsevier, Amsterdam.
8. Watts, A., and De Pont, J. J. H. H. M., Ed. (1986) *Progress in Lipid−Protein Interactions*, Vol. 2, Elsevier, Amsterdam.
9. Marsh, D., and Horváth, L. I. (1998) *Biochim. Biophys. Acta 1376*, 267−296.
10. Watts, A. (1998) *Biochim. Biophys Acta 1376*, 297−318.
11. White, S. H., and Wimley, W. C. (1998) *Biochim. Biophys. Acta 1376*, 339−352.
12. Killian, J. A. (1998) *Biochim. Biophys. Acta 1376*, 401−416.
13. Davis, J. M., Clare, D. M., Hodges, R. S., and Bloom, M. (1983) *Biochemistry 22*, 5298−5305.
14. Zhang, Y.-P., Lewis, R. N. A. H., Hodges, R. S., and McElhaney, R. N. (1992) *Biochemistry 31*, 11572−11578.
15. Zhang, Y.-P., Lewis, R. N. A. H., Hodges, R. S., and McElhaney, R. N. (1992) *Biochemistry 31*, 11579−11588.
16. Axelsen, P. H., Kaufman, B. K., McElhaney, R. N., and Lewis, R. N. A. H. (1995) *Biophys. J. 69*, 2770−2781.
17. Huschilt, J. C., Millman B. M., and Davis, J. H. (1989) *Biochim Biophys. Acta 979*, 139−141.
18. Bolen, E. J., and Holloway, P. W. (1990) *Biochemistry 29*, 9638−9643.
19. Huschilt, J. C., Hodges, R. S., and Davis, J. H. (1985) *Biochemistry 24*, 1377−1386.
20. Morrow, M. R., Huschilt, J. C., and Davis, J. H. (1985) *Biochemistry 24*, 5396−5406.
21. Zhang, Y.-P., Lewis, R. N. A. H., Hodges, R. S., and McElhaney, R. N. (1995) *Biophys. J. 68*, 847−857.
22. Pauls, K. P., MacKay, A. L., Soderman, O., Bloom, M., Taneja, A. K., and Hodges, R. S. (1985) *Eur. Biophys. J. 12*, 1−11,
23. Subczynski, W. K., Lewis, R. N. A. H., McElhaney, R. N., Hodges, R. S., Hyde, J. S., and Kusumi, A. (1998) *Biochemistry 37*, 3156−3164.
24. Zhang, Y.-P., Lewis, R. N. A. H., Henry, G. D., Sykes, B. D., Hodges, R. S., and McElhaney, R. N. (1995) *Biochemistry 34*, 2348−2361.
25. Zhang, Y.-P., Lewis, R. N. A. H., Hodges, R. S., and McElhaney, R. N. (1995) *Biochemistry 34*, 2362−2371.
26. Lewis, R. N. A. H., and McElhaney, R. N. (1993) *Biophys. J. 68*, 847−857.
27. Mantsch, H. H., Madec, C., Lewis, R. N. A. H., and McElhaney, R. N. (1985) *Biochemistry 24*, 2440−2446.
28. Lewis, R. N. A. H., and McElhaney, R. N. (1996) in *Infrared Spectroscopy of Biomolecules*, (Mantsch, H. H., and Chapman, D., Eds.) pp 159−202, John Wiley and Sons, New York.
29. Nagle, J. F. (1976) *J. Membr. Biol. 27*, 233−250.
30. Boggs, J. M. (1980) *Can. J. Biochem. 58*, 755−770.
31. Boggs, J. M. (1986) *Biochem. Cell. Biol. 64*, 50−57.
32. Boggs, J. M. (1987) *Biochim. Biophys. Acta 906*, 353−404.
33. Rinia, H. A., Kik, R. A., Demel, R. A., Snel, M. M. E., Killian, J. A., van der Eerden, J. P. J. M., and deKruijff, B. (2000) *Biochemistry 39*, 5852−5858.

BI002170U